Effect of Aluminum on the Local Structure of Silicon in Zeolites as Studied by Si K Edge X-ray Absorption Near-Edge Fine Structure: Spectra Simulation with a Non-Muffin Tin Atomic Background

Lusegen A. Bugaev,*[,†] Jeroen A. van Bokhoven,[‡] Valerii V. Khrapko,[†] Leon A. Avakyan,[†] and Jana V. Latokha[†]

Department of Physics, Southern Federal University, Zorge str., 5, 344090 Russia, and ETH Zurich, Institute for Chemical and Bioengineering, ETH Zurich, HCI E127, 8093 Zurich, Switzerland

Received: November 7, 2008; Revised Manuscript Received: February 3, 2009

Experimental Si K edge X-ray absorption near-edge fine structure (XANES) of zeolite faujasite, mordenite, and beta are interpreted by means of the FEFF8 code, replacing the theoretical atomic background μ_0 by a background that was extracted from an experimental spectrum. To some extent, this diminished the effect of the inaccuracy introduced by the MT potential and accounted for the intrinsic loss of photoelectrons. The agreement of the theoretical and experimental spectra at energies above the white lines enabled us to identify structural distortion around silicon, which occurs with increasing aluminum content. The Si K edge XANES spectra are very sensitive to slight distortions in the silicon coordination. Placing an aluminum atom on a nearest neighboring T site causes a distortion in the silicon tetrahedron, shortening one of the silicon−oxygen bonds relative to the other three.

I. Introduction

Zeolites are crystalline silica−alumina porous structures that find wide application as adsorbents, ion exchangers, catalysts, and catalyst supports. The tetrahedrally coordinated aluminum and silicon atoms are bridged by oxygen atoms; for each aluminum atom in the framework, there must be a cationic charge in the pores. The charge-compensating cations can be exchanged and are responsible for the ion-exchange capacity of zeolites. When the charge is compensated by protons, bridging hydroxyl groups form, and the zeolite shows Brønsted acidity and is catalytically active in Brønsted acid-catalyzed reactions.

The effect of aluminum on the framework of zeolite structures has been studied by various experimental and theoretical methods.[1−4] Among the experimental techniques, X-ray absorption spectroscopy (XAS) is very effective for determining the local structure around an element, irrespective of the aggregation state of the sample.[5] X-ray absorption near-edge fine structure (XANES) is sensitive to slight structural distortions.[6−8] However, the interpretation of experimental XANES and the extraction of structural information are usually complicated, since at low photoelectron energy, multiple scattering (MS) processes, multielectron excitations, polarization effects, and the effects of potential for photoelectron scattering contribute significantly to the fine-structure of the spectrum.[9−11] Extensive work has been performed to generate methods to simulate XANES spectra and thus obtain structural information.[12,13] The local structure of aluminum in zeolites has been studied using XANES and EXAFS at the Al K edge.[14−20] Si K edge XANES however is much less employed. X-ray diffraction, nuclear magnetic resonance spectroscopy, and Al K edge XAS show that the framework becomes increasingly disordered with increasing Si/Al ratio. We studied the local silicon structure of zeolites of various structure types and with different Si/Al ratios. We performed full multiple scattering calculations using the FEFF8 code[21] to simulate the experimental spectra. Because of the muffin tin (MT) approximation,[5] which is used in FEFF8 to generate the photoelectron scattering potential and approximate account for the intrinsic and extrinsic losses,[22] this code may not be suitable to reproduce the Si K edge XANES spectra of the strongly covalent zeolite framework. We propose an approach that, at least in part, circumvents inaccuracies in the theoretical spectra because of the MT approximation and intrinsic losses of photoionization. The changes in the spectra of faujasite, mordenite, and beta, the latter two of which have various Si/Al ratios, are interpreted based on small distortions around the silicon atoms.

II. Experimental Section

NH_4-exchanged zeolite samples were synthesized and characterized according to standard methods as reported earlier.[23,24] Si K edge XANES spectra were recorded at Lucia beam line at the Swiss Light Source (SLS) in Villigen in Switzerland.[25] The SLS operated at 2.4 GeV with a ring current of 300 mA in top-up mode. A double crystal monochromator equipped with a pair of InSb crystals was used. The energy resolution after the monochromator was between 1−1.5 eV, and the spot size of the X-ray beam was 0.5 × 0.5 mm. The incident beam intensity was determined by measuring the total electron yield of a 200 nm thick titanium foil. Spectra were recorded in vacuum on diluted powder samples attached to a copper plate by means of fluorescence detection. The detector was a silicon drift detector, which has an energy resolution of about 130 eV at the Pd L_3 edge at a count rate of about 50 kHz.

III. Si K Edge XANES of Beta, Mordenite, and Faujasite

Figure 1 shows a comparison of the experimental Si K edge XANES spectra of zeolite beta (Si/Al = 100), mordenite (Si/Al = 15), and faujasite (Si/Al = 2.6) with theoretical spectra

* To whom correspondence should be addressed. E-mail: bugaev@sfedu.ru.
† Southern Federal University.
‡ Institute for Chemical and Bioengineering.

10.1021/jp8098285 CCC: $40.75
Published on Web 03/12/2009

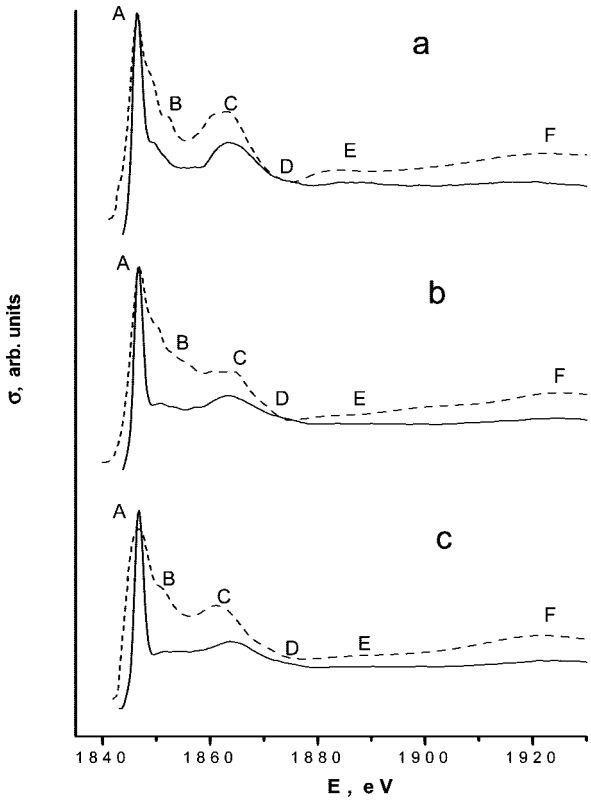

Figure 1. Experimental (solid lines) and theoretical (broken lines) Si K edge XANES spectra of the zeolites faujasite (Si/Al = 2.6) (a), mordenite (Si/Al = 15) (b), and beta (Si/Al = 100) (c).

calculated by the self-consistent field approximation and the complex Hedin−Lundqvist (HL) exchange-correlation potential.[26] The additional constant shift (vi0) 0.5 eV to a pure imaginary "optical" potential part was made to account for experimental broadening. Calculations were performed for the K edge, with the hole index 1 (tabulated core hole lifetime parameter), using the amplitude reduction factor $S_0^2 = 0.9$, the MT radii overlapping parameter of 1.3, and the value of Debye−Waller (DW) parameter $\sigma^2 = 0.005$ Å^2, typical for the room temperature.[27] The self-consistent potential was generated for the cluster radius of 3.3 Å to include the second coordination shell (first neighboring T-sites) of the absorbing silicon atom. Experimental and theoretical spectra are compared after aligning peak A. The very low content of aluminum in zeolite beta, with a Si/Al ratio of 100, enables the use of the crystal structure data of beta ($Si_{64}O_{128}$)[28] in the FEFF8 calculations. In this structure, the silicon atom is tetrahedrally coordinated to four oxygen atoms with approximately the same bond length of R_{Si-O} = 1.616 Å. The corresponding experimental Si K edge XANES are therefore considered to be a reference for the simulations of the Si K edge XANES spectra. The crystal structures of faujasite and mordenite were taken from the zeolite structural database[28] with the compositions [$Si_{192}O_{384}$] and $Na_8(H_2O)_{24}$-[$Si_{40}Al_8O_{96}$], respectively. For zeolite faujasite the replacements of some of the Si-atoms in the randomly chosen T sites by aluminum were made, so as to obtain varying Si/Al ratios.

According to the used structural data[28] the silicon atoms in each of the studied zeolites occupy a different nonequivalent crystallographic T-sites, and their numbers are one nonequivalent T-site in faujasite, six in mordenite, and nine in beta. For the considered zeolite these T-sites have the differences in radial distribution of the neighboring atoms, beginning from the second shell. Therefore, full multiple-scattering calculations for mordenite and beta were performed placing the absorbing Si atom in every nonequivalent site in the cell unit and using the clusters of radius R_{Si-O} = 6.5 Å (~70 atoms), which include the first- and the second-neighboring O tetrahedrons around the one with the absorbing silicon. A further increase in the size of the clusters did not effect the simulation. Comparison of $\chi(k)$ calculated for different nonequivalent sites in zeolite show that the main divergences in their features occur at the energies <1860 eV (region of B), while at the higher energies quite similar behavior is observed. As a result, theoretical Si K edge XANES spectra of mordenite and beta, presented in figure 1, were obtained by the average over the calculated $\chi(k)$ for all nonequivalent silicon sites in the unit cell.

All the experimental spectra showed a strong white line (feature A) with a small shoulder (feature B). There was a broad peak at about 20 eV above the adsorption edge (feature C), which is also observed in Al K edge spectra of tetrahedrally coordinated species and is typical of the tetrahedral coordination.[16,29] At higher energy, further features (D−F) were observed. The main difference between the spectra of the three different zeolites was found in the intensity and energy position of features B and C. The intensity decreased in the order of faujasite > mordenite > beta, which is also in the order of the increasing Si/Al ratio and of the decrease in the space group symmetry ($Fd\bar{3}m$ in faujasite to $Cmcm$ in mordenite to $P4_122$ in beta).

The theoretically calculated spectra show reasonable agreement with the experimental spectra above about 1855 eV. However, the width of the white line is overestimated, and features B−F generally show too high intensity. A different exchange-correlation potential with vi0 changed from 0.0 to 2.5 eV, with some variations: (i) in the size of the cluster around the absorbing Si from 4.3 Å (only first neighboring O tetrahedrons are included) to 7 Å, (ii) in the size of the self-consistency region for the potential, (iii) in the values of DW parameter σ^2 (from 0.002 to 0.2 Å^2), as well as the variations in the photoelectron mean free path and in the parameter for overlap of the neighboring MT spheres (from 1.0 to 1.5) did not significantly improve the agreement. This suggests that the lack of agreement probably originates mainly from the MT approximation used for the potential, which affects the ability to reproduce spectra of compounds with covalent silicon−oxygen bonds. These differences compared to experiment may also be due in part to the multielectron excitations, which are expected to be significant near to the adsorption edge.

To eliminate the influence of the MT approximation and the intrinsic losses, the calculated atomic background μ_0 was replaced in the expression $\mu = \mu_0(1 + \chi)^5$ by an atomic background that is extracted from experimental data according to a method proposed earlier.[30,31] In this method $\mu_0(k)$ is extracted from $\mu(k)$ using the criterion function with a set of parameters A, B, C, D, α, β, δ, and k^* to be determined

$$\mu_0(k) = \begin{cases} A\cdot[1/((k-\alpha)^2 + B^2) - 1/(\alpha^2 + B^2)], & k < k^* \\ C\cdot \arctan(\delta(k-\beta)) + D, & k > k^* \end{cases} \quad (1)$$

The number of independent parameters in eq 1 can be decreased using the continuity conditions at the boundary k^*, considered as an adjustable parameter also. The parameters in eq 1 are determined via the fit performed to meet the two following criteria: (1) coincidence of the Fourier transformations of functions $\mu(k)$ and $\mu_0(k)$ at low R region (<0.7 Å), and (2)

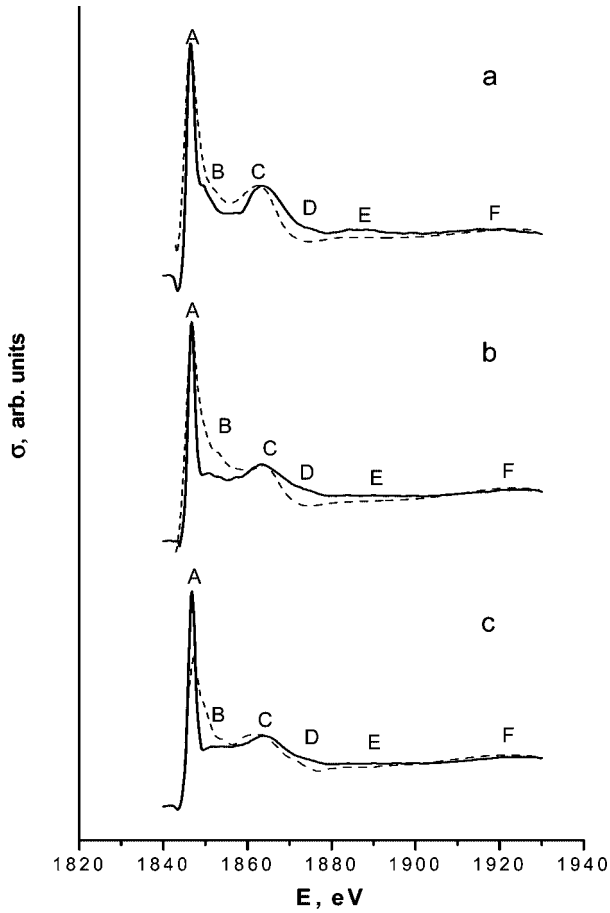

Figure 2. Si K edge XANES of the zeolites faujasite (Si/Al = 2.6) (a), mordenite (Si/Al = 15) (b), and beta (Si/Al = 100) (c) experimental spectra (solid lines) and theoretical spectra (broken lines), obtained by using μ_0 functions extracted from the experimental spectra.

coincidence of the convolutions of functions $\mu(k)$ and $\mu_0(k)$ with the Lorentzian broadening function assuming a large value of its energy width (~30 eV) to suppress $\chi(k)$ oscillations in the experimental spectrum.

The resulting Si K edge XANES spectra of zeolites faujasite, mordenite, and beta are presented in Figure 2. Replacing the theoretically calculated background did not have a significant effect on the spectra fine structure at energies higher than about 1855 eV; however, the intensity in this region was in better agreement with experiment. The most important improvement was in the white line, which was much narrower. At lower energy, the agreement between the theoretical and experimental spectra improved. The white line in the spectrum of faujasite was almost as narrow and intense as in the experimental spectrum. The intensity of feature B was more similar to the experimental spectrum. These characteristics were also true for the spectrum of mordenite, although feature B in the theoretical spectrum remained too intense and too broad. The new theoretical spectrum of beta showed a better overall intensity; however, the white line was still underestimated and was too broad, and feature B was still too intense. Using a non-MT absorption background $\mu_0(k)$ resulted in better agreement between theoretical and experimental spectra, especially for faujasite and to a lesser extent for mordenite and beta. The differences remained, especially for beta, because when we remove the effect of the MT potential inaccuracies in $\mu_0(k)$, their effect on the calculated photoelectron scattering phase-shifts, and hence on the $\chi(k)$ and on Si K edge XANES, remained and

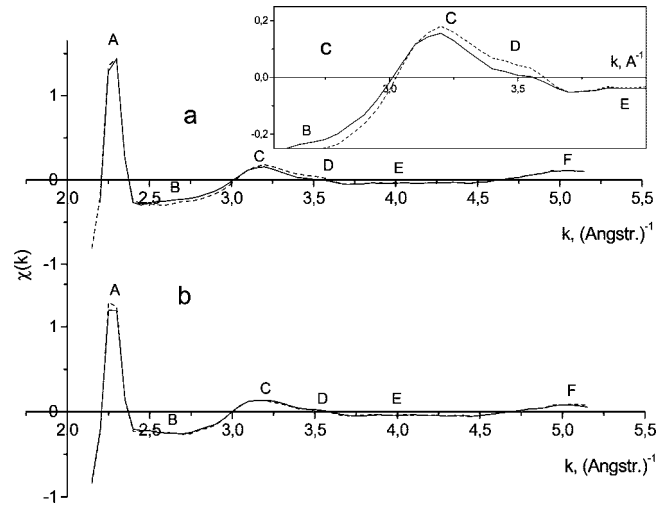

Figure 3. Comparison of $\chi(k)$ functions extracted from experimental Si K edge XANES in the zeolites (a) beta with Si/Al = 100 (solid line) and Si/Al = 12 (dotted line) as well as (b) mordenite with Si/Al = 15 (solid line) and Si/Al = 10 (dotted line). The insert (c) highlights the $\chi(k)$ for beta with Si/Al = 100 and 12 in the k range, where the difference in functions is observed.

increased with the space group symmetry decreasing from faujasite to beta.

The reasonable agreement of theoretical spectra with the experimental spectra at energies above the white lines ($E > 1855$ eV) means that, based on this spectral region, it is possible to establish the local structure of the silicon atoms in zeolites of different structure types and with different aluminum contents by analyzing the relative changes in Si K-edge XANES, calculated for alternative models of structural distortions.

IV. Analysis of Si K Edge XANES Spectra of Beta and Mordenite with Increasing Si/Al Ratio

Parts a and b of Figure 3 show the $\chi(k)$ of beta (Si/Al ratio of 100 and 12) and of mordenite (Si/Al ratio of 15 and 10). The functions were extracted from the experimental Si K edge XANES spectra by using $\chi(k) = \mu^{\text{exper}}(k)/\mu_0(k) - 1$, where $\mu_0(k)$ is the atomic background, which is proportional to the factorized "atomic" part of the absorption cross-section $\sigma_{\text{at}}(k)$.[32] $\mu_0(k)$ was extracted from the experimental spectrum.[30] The photoelectron wavenumber k is determined by the expression $k = (0.2625(E - E_{\text{MT}}))^{1/2}$, where the value of MT zero $E_{\text{MT}} = 1830$ eV is taken as the beginning of the k scale.

The $\chi(k)$ of mordenite with different Si/Al ratios (15 and 10) did not vary significantly, probably because of the limited variation in the ratio. The $\chi(k)$ of beta showed a small but significant variation in features B, C, and D. The white line and features E and F were insensitive to the Si/Al ratio.

Zeolite beta, with a Si/Al ratio of 12, contains silicon atoms with several aluminum atoms on the (next) nearest T sites. The modeling of the replacement of silicon atoms by aluminum in this structure is a complicated procedure, since the aluminum−oxygen bond is about 0.1 Å longer than the silicon−oxygen bond. Such elongation results in reconstruction of the local silicon environment and the appearance of structural distortions. Therefore, to establish the relationship of the observed changes in the Si K edge XANES between zeolite beta with Si/Al = 100 and 12 with these distortions the approach is employed which is related to the approaches effectively used for determination of local structural distortions[33,34] and relaxations around impurities.[35,36] In this approach the most plausible models for

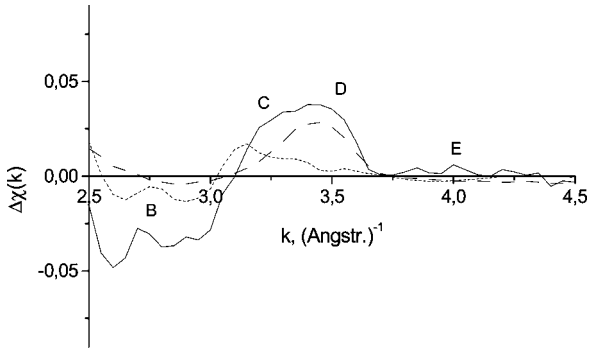

Figure 4. Comparison of the residual functions $\Delta\chi(k)$ in zeolite beta, which characterize the following differences: between experimental functions $\chi(k)$ of Si/Al = 100 and 12 (solid line); between theoretical $\chi(k)$ calculated in reference structure of beta Si/Al = 100 and (a) $\chi(k)$ calculated in assumption of O_4 tetrahedron distortion around the absorbing Si according to (1 + 3) radial distribution model and under the fixed positions of other atoms (long dotted line), (b) $\chi(k)$ calculated in assumption of a rigid O_4 tetrahedron for the absorbing Si, which has, among the four neighboring tetrahedrons, one with aluminum, located at R_{Si-Si} + 0.2 Å to provide the normal R_{Al-O} = 1.72 Å (short dotted line).

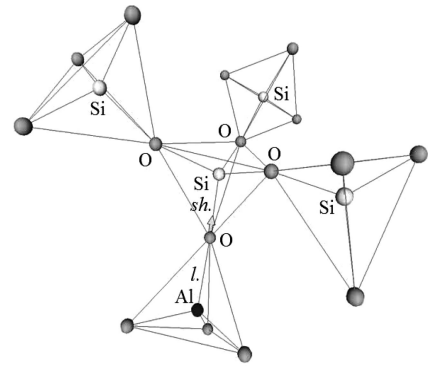

Figure 5. Silicon local structure in zeolite beta, distorted by the presence of aluminum in one of the first-neighboring O tetrahedrons to the absorbing Si. The shortened and elongated bonds are marked by "sh" and "l," respectively.

the local structure of silicon were generated by systematically changing the reference structure of zeolite beta and comparing the changes in theoretical Si K edge XANES, calculated by these models, with the differences in experimental spectra of beta with Si/Al = 100 and 12. To generate these models some silicon atoms were replaced by aluminum atoms with an aluminum−oxygen bond length of 1.72 Å. Meanwhile, the aluminum oxygen tetrahedrons were additionally displaced by about 0.2 Å relative to the absorbing silicon atom. Finally, the simulations were performed by assuming that the silicon oxide tetrahedron was either symmetric or distorted. A distortion model in which silicon was surrounded by three oxygen atoms at the normal distance of R_{Si-O} = 1.62 Å and one oxygen at a shortened distance of R_{Si-O} = 1.55 Å showed the best agreement with the experiment. In the model, we assume that the three silicon−oxygen bonds, belonging to Si−O−Si chains, have a distance of $R_{Si-O} \approx$ 1.62 Å, and the silicon−oxygen and aluminum−oxygen bonds in a Si−O−Al chain R_{Si-O} = 1.55 Å and R_{Al-O} = 1.71 Å. Such a distortion model originated from the theoretically obtained coordinates of silicon, oxygen, and aluminum atoms in H-Fer zeolites.[37] Furthermore, a (1 + 3) distortion model is suggested by XRD data for Na mordenite with the composition $Na_8(H_2O)_{25}Si_{40}Al_8O_{96}$,[27] which showed that there are four different T sites for silicon atoms in this structure and that two of them show one shortened distance and threes show approximately normal Si−O distances. The effect of some alternative structural changes in silicon local structure in zeolite beta on the B−E features of $\chi(k)$ is illustrated in Figure 4. The residual function $\Delta\chi(k)$ for experimental spectra of beta (Si/Al = 100) and (Si/Al = 12) was obtained aligning the peaks A, and the same aligning is used for the comparison of theoretical functions $\Delta\chi(k)$ with the experimental one, which is validated by the stable energy position of peak A in both experimental Si K edge XANES of beta.

The simulations of $\chi(k)$ for zeolite beta (Si/Al = 12) in the considered models indicates that the spectra were unaffected at an energy higher than 1885 eV ($k > 4.0$ Å^{-1}). By assumption of a rigid silicon oxide tetrahedron, the replacement of silicon by aluminum in the first neighboring T sites effected the B feature and the low-energy shoulder of peak C. The corresponding residual function $\Delta\chi(k)$ in Figure 4, which represents the result of Si−Al distance elongation by 0.2 Å, does not explain the experimental curve in the C−D region, but the position of its peak at ∼3.15 Å correlates with the Natoli rule,[38] though this peak is formed not by the Si(Al) atoms only. Simulations of $\chi(k)$ show that the second neighboring Al can contribute essentially into the C−D region at $k > 3.25$ Å if the Si−Al distance could be decreased by not less than 0.2 Å compared to the Si−Si one in the reference structure of beta. By assumption of a rigid O_4 tetrahedron around the absorbing Si, this can occur only if the bond angle ∠(Si−O−Al) in the Si−O−Al chain can be decreased by ≥30°, which is not observed in the spread of the Si−O−Si(Al) angles in NMR experiments for zeolites at the high aluminum contents.

The replacement of silicon by aluminum in the next neighboring T sites (at $R_{Si-T} \approx$ 4.5 Å) were seen in the region of feature B. Figure 4 shows that the difference between $\chi(k)$ of a rigid O_4 tetrahedron model and that of the distorted one is quite similar to the difference in the experimental spectra of beta with an Si/Al ratio of 100 and 12, which suggests a similar origin. The presence of aluminum in the second coordination shell of silicon distorts the silicon oxygen tetrahedron as illustrated in Figure 5, which is visible in the XANES fine structure.

V. Summary and Conclusions

FEFF8 simulations of the Si K edge XANES spectra of the zeolites faujasite, mordenite, and beta and the analysis of changes in experimental $\chi(k)$ of zeolite beta with Si/Al = 100 and 12 lead to the following conclusions:

(1) The effects of the potential inaccuracy of the MT approximation and the photoelectron intrinsic losses in the FEFF8 calculations of Si K edge XANES for the studied zeolites became fewer at energies above 1855 eV by replacing the calculated atomic background μ_0 by the corresponding function extracted from the experimental spectrum. Differences between the theoretical and experimental spectra remain.

(2) The fairly good agreement of theoretical and experimental spectra at energies >1855 eV, resulting from this replacement, enabled the implementation of the FEFF8 simulations of χ functions for the different, most plausible models of the local structure of silicon distortions in zeolite Beta (Si/Al = 12).

(3) The presence of an aluminum atom on a neighboring T site distorts the silicon tetrahedron, i.e., shortens one of the silicon−oxygen bonds.

Acknowledgment. J.Av.B. thanks the Swiss National Science Foundation and LABORATORY the Southern Federal University for financial support. These experiments were performed

on the LUCIA beamline at the Swiss Light Source, Paul Scherrer Institut, Villigen, Switzerland.

References and Notes

(1) Melchior, M. T.; Vaughan, D. E. W.; Jarman, R. H.; Jacobson, A. J. *Nature* **1982**, *298*, 455.

(2) Kokotailo, G. T.; Fyfe, C. A. *Rigaku J.* **1995**, *12*, 3.

(3) Sohn, J. R.; De Canio, S. J.; Lunsford, J. H. *Zeolites* **1986**, *6*, 225.

(4) Ivanova, E. A.; Shor, A. M.; Nasluzov, V. A.; Vayssilov, G. N.; Rosch, N. *J. Chem. Theory Comput.* **2005**, *1*, 459.

(5) Koningsberger, D. C.; Prins, R. *SEXAFS and XANES*; Wiley: New York, 1988.

(6) Daniel, R.; Cormier, L.; Roux, J.; Henderson, G. S.; de Ligny, D.; Flank, A. M.; Lagarde, P. *AIP Conf. Proc.* **2007**, *882*, 419.

(7) Rulis, P.; Yao, H.; Ouyang, L.; Ching, W. Y. *Phys. Rev. B* **2007**, *76*, 245410.

(8) Souza-Neto, N. M.; Ramos, A. Y.; Tolentino, H. C. N.; Favre-Nicolin, E.; Ranno, L. *Phys. Rev. B* **2004**, *70*, 174451.

(9) Bugaev, L. A.; Gegusin, I. I.; Datshyuk, V. N.; Novakovich, A. A.; Vedrinskii, R. V. *Phys. Status Solidi B* **1986**, *133*, 195.

(10) Joly, Y. *Phys. Rev. B* **1996**, *53*, 13029.

(11) Rehr, J. J.; Kas, J. J.; Prange, M. P.; Sorini, A. P.; Campbell, L. W.; Vila, F. D. *AIP Conf. Proc.* **2007**, *882*, 85.

(12) Benfato, M.; Della, Longa; D'Angelo, P. *Phys. Scripta* **2005**, *T115*, 28.

(13) Smolentsev, G.; Soldatov, A. V.; Feiters, M. C. *Phys. Rev. B.* **2007**, *75*, 144106.

(14) Koningsberger, D. C.; Miller, J. T. *Catal. Lett.* **1994**, *29*, 77.

(15) van Bokhoven, J. A.; Sambe, H.; Ramaker, D. E.; Koningsberger, D. C. *J. Phys. Chem.* **1999**, *103*, 7557.

(16) van Bokhoven, J. A.; Nabi, T.; Ramaker, D. E.; Koningsberger, D. C. *J. Phys.: Condens Matter.* **2001**, *13*, 10247.

(17) van Bokhoven, J. A.; Kunkeler, P. J.; van Bekkum, H.; Koningsberger, D. C. *J. Catal.* **2002**, *211*, 540.

(18) van Bokhoven, J. A.; van der Eerden, A. M. J.; Prins, R. *J. Am. Chem. Soc.* **2004**, *2*, 4506.

(19) Joyner, R. W.; Smith, A. D.; Stockenhuber, M.; van den Berg, M. W. E. *Phys. Chem. Chem. Phys.* **2004**, *6*, 5435.

(20) Drake, I. J.; Zhang, Y. H.; Gilles, M. K.; Liu, C. N. T.; Nachimuthu, P.; Perera, R. C. C.; Wakita, H.; Bell, A. T. *J. Phys. Chem. B* **2006**, *110*, 11665.

(21) Ankudinov, L.; Ravel, B.; Rehr, J. J.; Conradson, S. D. *Phys. Rev. B.* **1998**, *58*, 7565.

(22) Rehr, J. J.; Albers, R. C. *Rev. Mod. Phys.* **2000**, *72*, 621.

(23) Abraham, A.; Lee, S.-H.; Shin, C.-H.; Hong, S. B.; Prins, R.; van Bokhoven, J. A. *Phys. Chem. Chem. Phys.* **2004**, *6*, 3031.

(24) Xu, B.; Sievers, C.; Hong, S. B.; Prins, R.; van Bokhoven, J. A. *J. Catal.* **2006**, *244*, 163.

(25) Flank, A.; Cauchon, G.; Lagarde, P.; Bac, S.; Janousch, M.; Wetter, R.; Dubuisson, J.; Idir, M.; Langlois, F.; Moreno, T.; Vantelon, D. *Nucl. Instr. Meth.* **2006**, 246.

(26) Hedin, L.; Lundqvist, S. *J. Phys. C* **1971**, *4*, 2064.

(27) Bugaev, L. A.; van Bokhoven, J. A.; Sokolenko, A. P.; Latokha, Ya. V.; Avakyan, L. A. *J. Phys. Chem. B.* **2005**, *109*, 10771.

(28) Database of Zeolite Structures, http://www.iza-structure.org/databases/.

(29) van Bokhoven, J. A. *Phys. Scripta* **2005**, *T115*, 76.

(30) Bugaev, L. A.; Sokolenko, A. P.; Dmitrienko, H. V.; Flank, A. M. *Phys. Rev. B* **2002**, *65*, 024105.

(31) Bugaev, L. A.; van Bokhoven, J. A.; Avakyan, L. A.; Latokha, Ya. V. *Amer. Inst. Phys.* **2007**, *882*, 117 Conf. Proc. .

(32) Borovskii, I. B.; Vedrinskii, R. V.; Kraizman, V. L.; Sachenko, V. P. *Uspekhi Fiz. Nauk.* **1986**, *149*, 275.

(33) Benfatto, M.; Della Longa, S. *J. Synchrotron Radiat.* **2001**, *8*, 1087.

(34) Merkling, P. J.; Munoz, A.; Pappalardo, R. R.; Marcos, E. S. *Phys. Rev. B* **2001**, *64*, 092201.

(35) Gaudry, E.; Cabaret, D.; Brouder, C.; Letard, I.; Rogalev, A.; Wilhlem, F.; Jaouen, N.; Sainctavit, Ph. *Phys. Rev. B* **2007**, *76*, 094110.

(36) Juhin, A.; Calas, G.; Cabaret, D.; Galoisy, L.; Hazemann, J.-L. *Am. Mineral.* **2008**, *93*, 800.

(37) Nieminen, V.; Sierka, M.; Murzin, D. Y.; Sauer, J. *J. Catal.* **2005**, *231*, 393.

(38) Wu, Z. Y.; Gota, S.; Jollet, F.; Pollak, M.; Gautier-Soyer, M.; Natoli, C. R. *Phys. Rev. B* **1997**, *55*, 2570.

JP8098285